Defining the mechanism of PDI interaction with disulfide-free amyloidogenic proteins: implications for exogenous protein expression and neurodegenerative disease

Pingyu Yan[1#], Zhiyuan Zou[1#], Shiyao Zhang[1#], Rui Wang[1], Tingting Niu[1], Xia Zhang[1], Defu Liu[1], Xuejie Zhou[1], Alan K Chang[2], Nathaniel G N Milton[3], Gary W Jones[3] and Jianwei He[1]*

[1]School of Life Science, Liaoning University, Shenyang 110036, China;

[2] College of Life and Environmental Sciences, Wenzhou University, Wenzhou, 325035, China

[3]Centre for Biomedical Science Research, School of Clinical and Applied Sciences, Leeds Beckett University, City Campus, Leeds LS1 3HE, United Kingdom

[#]These authors contributed equally to this work.

*Corresponding author. Email: jwhe@lnu.edu.cn;

Key words

Protein disulfide isomerase; amyloidogenic protein; Molecular chaperone

Acknowledgements

We thank Xin Deng and Hailong Li for proteomics data processing and repository assistance, we are grateful to Linan Xu for critical discussion on *in silico* studies. This work was supported by grants from National Natural Science Foundation of China (No. 31670103).

Abstract

Protein disulfide isomerase (PDI) is an important molecular chaperone capable of facilitating protein folding in addition to catalyzing the formation of a disulfide bond. To better understand the distinct substrate-screening principles of *Pichia pastoris* PDI (Protein disulfide isomerase) and the protective role of PDI in amyloidogenic diseases, we investigated the expression abundance and intracellular retention levels of three archetypal amyloidogenic disulfide bond-free proteins (Aβ42, α-synuclein (α-Syn) and SAA1) in *P. pastoris* GS115 strain without and with the overexpression of

PpPDI (*P. pastoris* PDI). Intriguingly, amyloidogenic Aβ42 and α-Syn were detected only as intracellular proteins whereas amyloidogenic SAA1 was detected both as intracellular and extracellular proteins when these proteins were expressed in the PpPDI-overexpressing GS115 strain. The binding between PpPDI and each of the three amyloidogenic proteins was investigated by molecular docking and simulations. Three different patterns of PpPDI-substrate complexes were observed, suggesting that multiple modes of binding might exist for the binding between PpPDI and its amyloidogenic protein substrates, and this could represent different specificities and affinities of PpPDI towards its substrates. Further analysis of the proteomics data and functional annotations indicated that PpPDI could eliminate the need for misfolded proteins to be partitioned in ER-associated compartments.

1. Introduction

Protein disulfide isomerase (PDI) is an important molecular chaperone capable of facilitating protein folding in addition to catalyzing the formation of a disulfide bond. It is essential for the accurate and efficient co-translational and post-translational folding of secreted proteins. PDI adopts a U-shaped domain arrangement in which four thioredoxin-like domains (termed a, b, b', and a'), a linker (x), and a C-terminal extension domain (c) are arranged in the order a-b-b'-x-a'-c (Fig. 1)[1]. While the domains a and a' are mainly responsible for catalyzing the thiol-disulfide exchange reactions, domains b and b' have been suggested to contribute to the molecular chaperone activity of PDI [2]. The b and b' domains provide a large hydrophobic pocket that binds with a wide variety of peptides and misfolded proteins in a reversible manner [3-7]. In particular, the b' domain has been widely demonstrated to significantly improve the activity of PDI toward misfolded protein substrates [8-10].

A number of studies have shown that the overexpression of PpPDI can increase the secretion of exogenous recombinant proteins in the yeast *Pichia pastoris* [11-13]. However, overexpression of PpPDI alone does not always increase the expression levels of all foreign proteins [14]. Additionally, these studies have mainly focused on disulfide-containing or disulfide-rich proteins, with little research looking at the effect of PpPDI on the expression of disulfide-free proteins. This is of great importance since recent structural and functional studies have demonstrated that PDI members not only play an essential role in proteostasis in the ER but also exert diverse effects on the development of numerous human disorders, which include cancer and neurodegenerative diseases (Parkinson's or Alzheimer's) [15, 16].

Pichia pastoris is a popular host for heterologous protein expression in research and industry, with over 800 recombinant proteins having been produced using this system [11]. The availability of complete genome sequence combined with a well-established genetic engineering methodology and the non-pathogenic nature of *P. pastoris* have made this organism an ideal model system for the production of recombinant proteins, both for therapeutic drugs and vaccines [17]. To improve the expression efficiency of foreign proteins, further investigation is required to better understand the mechanisms by which endogenous molecular chaperones efficiently capture diverse misfolded clients and help with the folding of various substrate proteins.

In this study, three representative disulfide-free amyloidogenic proteins were employed as client-substrates to define the distinct client-recruiting system of PpPDI for disulfide-free proteins. These were (i) amyloid-β (Aβ) 42, (ii) human serum amyloid A1 (SAA1) and (iii) α-synuclein (α-Syn). The Aβ peptide is a short peptide that exists in several forms, primarily ranging from 37 to 43 amino acids. These peptides are the main components of the amyloid plaques found in the brain of patients with Alzheimer's disease (AD) and they play a central role in the pathology of the disease. Although Aβ40

is the main form of Aβ peptide, the longer Aβ42 is pathologically more important because of its much greater toxicity compared with Aβ40. The abnormal aggregation of Aβ42 and the accumulation of Aβ42 plaques are an indicator of progressive AD status [18-20]. Serum amyloid A (SAA) is a major serum acute-phase protein and a cause of secondary amyloidosis [21]. Since SAA1 deposits can cause inflammatory amyloidosis, it has become a reliable biomarker for inflammatory diseases, chronic metabolic disorders and advanced malignancies [22-25]. α-Syn is a disulfide-free amyloidogenic protein related to the pathogenesis of Parkinson's disease [26, 27]. Thus, biochemical, proteomic and molecular modelling approaches were used to investigate how PpPDI interacts with disulfide-free protein substrates. The findings obtained might provide new insight into the functioning of this important molecular chaperone. This might also provide a way to improve the strategies for increasing the expression of exogenous proteins in commercial *Pichia* strains and to establish PDI as a genuine therapeutic target for neurodegenerative diseases.

2. Materials and methods

2.1 Experimental Design and Statistical Rationale

The experimental design and statistical rationale for each of the experiments conducted in this study are described in detail in each subsection and figure legend. In brief, we first aimed to characterize the protein expression profiles of three model amyloidogenic disulfide-free proteins (Aβ42, SAA1, α-Syn). The secretion of the three recombinant disulfide-free amyloidogenic proteins by *P. pastoris* GS115 and *P. pastoris* GS115 that overexpressed PpPDI (GS115-PpPDI) was examined by measuring the levels of their secreted forms. Moreover, co-IP and molecular modelling approaches were used to investigate how PpPDI might interact with disulfide-free protein substrates. Next, *P. pastoris* GS115 expressing Aβ42/SAA1/α-syn and GS115 expressing both PpPDI and

Aβ42/SAA1/α-syn, were subjected to proteome profiling. PSM FDR≤0.01 and Protein FDR≤0.01 were used to screen the mass spectrometry data for peptide and protein identification, respectively.

2.2 Strains and plasmids

The plasmid vectors pPICZα A and pPIC3.5K were purchased from Invitrogen. *Pichia pastoris* GS115 was provided by Shutao Liu at Fuzhou University, China.

2.3 Antibodies

The DNA sequences encoding Aβ42, SAA1 and α-Syn were synthesized by Nanjing Kingsray Biotechnology Company. Anti-Aβ42 antibody (0.2 mg/mL), anti-SAA1 antibody (0.1 mg/mL) and anti-α-Syn antibody (0.2 mg/mL) were obtained from Santa Cruz. Goat anti-mouse antibody was obtained from Real-Times (Beijing) Biotechnology, Co., Ltd.

2.4 Constructs and Protein Production.

To construct a PpPDI over-expressing *P. pastoris* strain, the *PpPDI* gene (GenBank EU805807) was amplified from the chromosomal DNA of the wild-type strain, *P. Pastoris* strain X33 (Invitrogen), based on a published sequence [14, 28]. The DNA encoding the full-length *PpPDI* was inserted into the expression vector pPIC3.5K under the control of the *AOX1* promoter, yielding pPIC3.5K-*PpPDI*. The plasmid pPIC3.5K-*PpPDI* was linearized with *Sac* I and then introduced into *P. pastoris* GS115 by electroporation. Positive transformants were selected and their genomic DNA was isolated and screened for the presence of the *PpPDI* gene by PCR.

The codon of the DNA encoding Aβ42/SAA1/α-Syn was optimized according to the codon usage of *P. pastoris*, making it more suitable for expression in *P. pastoris*. The codon-optimized sequence of Aβ42/SAA1/α-Syn was inserted into the plasmid pPICZαA. The identities of the inserted sequences in these constructs were verified by DNA sequencing. The constructs were then linearized with *Sac*1, and each linearized construct was subsequently introduced into competent cells prepared

from the PpPDI over-expressing GS115 strain as well as the normal GS115 strain by electroporation. PCR screening was used to verify the presence of the inserted genes in the positive clones. The expression of the proteins was induced by methanol for 72 h at 30 ℃.

2.5 Cytoplasmic protein extraction from *P. pastoris*

The yeast cells were harvested by centrifugation at 4,000 × *g* for 10 min at 4℃ after 72 h of induction by methanol. The collected cells were twice resuspended in ice-cold deionized water followed by centrifugation at 8,000 × *g* for 2 min, and the resulting cell pellet was treated with Yeast Protein Extraction Reagent (Takara) to release the intracellular proteins. For extracellular protein sample preparation, the yeast cultures were centrifuged at 1,900 × *g* and 4℃ for 10 min to pellet the cells, and the supernatant was further centrifuged at 8,000 × *g* and 4℃ for 30 min to remove any insoluble protein aggregates. The supernatant was used for extracellular protein analysis. All protein samples were treated with SDS-PAGE sample-loading buffer at 100℃ for 5 min and stored at −80℃ for SDS-PAGE and Western blotting analysis.

2.6 Co – IP and Western blot analysis

The cell pellet was washed with ice-cold PBS buffer and lysed in Lysis/Equilibration Buffer (Capturem IP & Co-IP Kit, Clontech) containing a mixture of protease inhibitors using 200 μL of the buffer per 1×10^6 cells. The sample was incubated on ice for 30 min and then centrifuged at 17,000 × *g* for 10 min to collect the supernatant. One milligram lysate was incubated with the appropriate amount of antibody (anti-Aβ42 or anti-SAA1) at 4℃ for 1.5 h. The sample was collected on a spin column and subjected to SDS-PAGE. After that, the proteins in the gel were transferred to a PVDF membrane. The membrane was blocked with Tris-buffered saline (TBS) solution containing 5% non-fat milk and 0.05% Tween 20 (TBST) at room temperature (RT) for 2 h. This was followed by incubation with the desired primary antibody at 4℃ for overnight, and then with the appropriate

secondary antibody at room temperature for 2 h. After that, the membrane was washed four times with TBST and then subjected to chemiluminescence assay.

2.7 LC-MS /MS sample preparation and measurement

An aliquot (70 μL) of SDT lysate (4% SDS, 100 mM DTT, 100 mM Tris-HCl) and 1M DTT (final concentration 100 mM) were added to the sample followed by centrifugation at 2,500 × g and 4℃ for 5 min and heating at 100ºC for 5 min. The FASP method was used for proteolysis. The peptides derived from enzymatic hydrolysis were desalted and vacuum-dried using a C18 StageTip. After drying, the peptides were re-dissolved in 0.1% TFA and the peptide concentration was determined by absorbance at 280 nm before LC-MS analysis.

An appropriate amount of peptide was chromatographed using a nanoliter flow rate Easy nLC 1200 chromatography system (Thermo Scientific). Solution A consisted of 0.1% aqueous formic acid, and solution B consisted of 0.1% formic acid, acetonitrile and water (95% of acetonitrile). The column was equilibrated with 100% solution A. The sample was injected into a Trap Column (100 μm * 20 mm, 5 μm, C_{18}, Dr. Maisch GmbH) and allowed to run through a separating column (75 μm × 150 mm, 3μm, C_{18}, Dr. Maisch GmbH) via gradient elution at a flow rate of 300 nL/min. The column was eluted with a gradient consisting of solution A and solution B as follows: 0 minutes---3 minutes, linear gradient of solution B from 2% to 7%; 3 minutes---48 minutes, linear gradient of solution B from 7% to 35%; 48 minutes---53 In minutes, the linear gradient of solution B is from 35% to 90%; in 53 minutes----60 minutes, the solution B is maintained at 90%. The separated peptides were subjected to DDA (data-dependent acquisition) mass spectrometry using a Q-Exactive Plus mass spectrometer (Thermo Scientific). The analysis time was 60 min. Detection was set to a positive ion mode with a parent ion scanning range from 300 to 1800 m/z, and a primary mass spectrometer resolution of 70,000 @m/z 200, AGC target of 1e6, and a primary Maximum IT of 50 ms. Peptide

secondary mass spectrometry was performed as follows: A full mass spectrum of the 20 highest intensity parent ions (MS2 scan) was acquired after each full scan, and under the following parameter settings: resolution of the second mass spectrum - 17,500 @ m/z 200; AGC target - 1e5; Level 2 Maximum IT - 50 ms; MS2 Activation Type - HCD; Isolation window - 2.0 Th; Normalized collision energy - 27.

The mass spectrometry proteomics data have been deposited to the ProteomeXchange Consortium via the PRIDE [29] partner repository with the dataset identifier PXD021130.

2.8 Database searching and data analysis

For the proteome of *P. pastoris* GS115 that overexpressed Aβ42, α-Syn or SAA1, both without and with PpPDI overexpression, MaxQuant version 1.6.1.0 MS Database retrieval software was used to process the raw MS data, and Uniprot Protein Database was used to compare the sequences from *Homo sapiens* (169753 Protein sequences in total) with those from *P. pastoris* (5256 Protein sequences in total). Enzyme specificity was set to trypsin, and the search included cysteine carbamidomethylation as a fixed modification and N-acetylation of protein and oxidation of methionine as variable modifications. Up to two missed cleavages were allowed for protease digestion. MaxQuant uses individual mass tolerances for each peptide, but the initial maximum precursor mass tolerances were set to 20 ppm in the first search and 4.5 ppm in the main search, and the fragment mass tolerance was set to 20 ppm. The false discovery rate was controlled with a target-decoy approach at less than 1% for peptide spectrum matches and less than 1% for protein group identifications.

Gene ontology (GO) enrichment analysis was performed online at http://omicslab.genetics.ac.cn/GOEAST/index.php by a default procedure without adopting a multi-test adjustment method. The P-value of the significance for the enrichment was less than 0.01.

2.9 Docking

The protein-protein complex was predicted using an online ZDOCK server (http://zdock.umassmed.edu/). Briefly**,** the appropriate PDB files were uploaded to the ZDOCK server. Two hundred complexes were automatically predicted and the one with the highest score was used for further molecular dynamic study according to a previously reported method [30].

2.10 Molecular dynamic simulation

All the 3D structures of the proteins used in this study were obtained from RSCB (Protein Data Bank, PDB). The $A\beta_{42}$ monomer (PDB: 1Z0Q) was presented as an aqueous solution structure of Aβ Peptide (1-42). NotePad++ software was employed to obtain a SAA1 monomer from an X-ray tetramer (PDB: 4IP8). The structures of α-Syn (PDB:1XQ8) and PpPDI (PDB: 2B5E) were obtained from solution NMR and X-ray diffraction, respectively.

All simulations were performed with the GROMACS 5.1.2 software package with a constant number, pressure, temperature and periodic boundary conditions. Each complex was immersed in the cubic boxes filled with spc216 water with a 1-nm distance between protein and box edges. The GROMOS96 54a7 force field was applied in all simulations. The linear constraint solver (LINCS) method was used to constrain bond lengths, allowing for an integration step of 2 fs. The temperature and pressure were coupled using V-rescale and Parrinello-Rahman algorithm, respectively. The solvated system was first neutralized by adding Na^+ or Cl^- into the solvent, and energy minimization was then performed using the Steepest Descent algorithm to reach a stable state with the lowest entropy. The backbone atoms of the structure were then fixed, while the side chains and solvent were allowed to move without restraint for 500 ps. After equilibration, several independent simulations were carried out over a 20-ns period and at 300 K, pH 7.0 and 1 bar pressure. The coordinate trajectories were saved every 1 ps for subsequent data analysis.

3. Results

3.1 Analysis of disulfide-free amyloidogenic proteins expressed in *P. pastoris*

The secretion of three recombinant disulfide-free amyloidogenic proteins expressed in *P. pastoris* GS115 and *P. pastoris* GS115 that overexpressed PpPDI (GS115-PpPDI) was examined after 3 days of cultivation when the secreted proteins reached maximum levels (Fig. 2). Western blot analysis revealed no detectable naturally disordered Aβ42 and α-Syn in the culture supernatants of both GS115 and GS115-PpPDI (Fig. S1A & S1B). This indicated that the nascent Aβ42 and α-Syn were unstable and they either unfolded or aggregated so that no correctly folded protein was detected in the culture medium. As expected, the intracellular retention of Aβ42 and α-Syn were detected in both GS115 and GS115-PpPDI cell extracts (Fig. 2A&B). The retention levels of the two proteins in the cell extract of GS115-PpPDI were higher than those detected in the cell extract of GS115. The discrepancy in protein retention level between GS115-PpPDI and GS115 was even greater for Aβ42 than for α-Syn (Fig. 2A). Moreover, western blot clearly detected the presence of α-Syn dimer in both GS115 and GS115-PpPDI cell extracts (Fig. 2B), indicating an obvious preference for α-Syn to form a dimer. Compared with Aβ42 and α-Syn, the remaining amyloidogenic protein, SAA1, was found secreted in the culture supernatants of both GS115 and GS115-PpPDI (Fig. 2C). Interestingly, in contrast to the observations of Aβ42 and α-Syn, both intracellular retention and expression level of SAA1 in GS115 were slightly higher than those observed for GS115-PpPDI (Figs. 2C & D). The results suggested that overexpression of PpPDI could significantly increase the intracellular retention of naturally disordered amyloidogenic proteins (Aβ42 and α-Syn) but had no obvious effect on the retention of SAA1, which is an intrinsically structured protein. The overexpression of PpPDI might therefore have a different effect on the expression of exogenous disulfide-free proteins in *P. pastoris*.

Subsequently, co-immunoprecipitation (co-IP) was performed to identify the relevant intracellular PpPDI–amyloidogenic protein interaction. The cell extract was immunoprecipitated with a PpPDI-specific antibody and the bound proteins were then probed with an antibody specific for each of the amyloidogenic proteins or vice versa. Unfortunately, the co-IP experiments only revealed positive interaction between PpPDI and Aβ42, and in the GS115-PpPDI cell extract. While the co-IP methodology is straightforward, identifying intracellular PpPDI–substrate interactions could be difficult because of the nature of the interaction (PpPDI is a molecular chaperone), nonspecific binding to IP components and antibody contamination, all of which could mask the detection. In addition, the western blot and co-IP results suggested that PpPDI might bind to each of the tested amyloidogenic proteins with a different affinity. Therefore, to investigate this hypothesis, a combined method consisting of co-IP followed by LC-MS/MS was used to examine the weak association between PpPDI and the amyloidogenic proteins. At the same time, both *in silico* analysis and molecular dynamics (MD) simulations were performed to determine the possible binding mode that governs the binding between PpPDI and each of the three amyloidogenic proteins.

3.2 Docking analysis of the binding of PpPDI with three amyloidogenic disulfide-free proteins

To investigate how PpPDI may interact with the amyloidogenic substrates, docking simulations between these two molecules were performed. Interestingly, the predicted mode of binding differed among the three pairs of proteins. Aβ42 and α-Syn were found in the central cleft of the U-shaped PpPDI molecule (Fig. 3A & 3B). Aβ42 appeared to bind to the a and b’ domains of PpPDI whereas α-Syn seemed to clamp the U-shaped structure of PpPDI like a "clip", with the a, b and b’ domains of PpPDI included in the binding site for α-Syn. The interacting residues of the possible binding pattern and properties resulting from the binding are listed in Supplementary Table 1 and Table 2. The interacting residues of Aβ42 were mainly residue 11 to 42, which have been demonstrated to

play an important role in the amyloidogenic progress. PpPDI formed more hydrogen bonds with Aβ42 or α-Syn than with SAA1 (red dotted line in Fig. 3A & 3B). SAA1 did not enter the U-shaped groove of PpPDI. It was instead bound to the a' and b' domains of PpPDI from the outside (Fig. 3C). Furthermore, there was no hydrogen bond between the two proteins, only hydrophobic interaction. The specific residues involved in hydrophobic interactions are shown in Supplementary Table 3. The results from docking simulations suggested that multiple possibilities might exist for the binding between PpPDI and these amylodiogenic proteins, leading to different specificities and affinities of PpPDI toward its substrates.

The data obtained from LC-MS/MS analysis confirmed that the presence of PpPDI could be detected in the proteins immunoprecipitated from the cell lysate of GS115-PpPDI expressing Aβ42, α-Syn or SAA1. In comparison, PpPDI was not detected in the 103 identified SAA1-interacting proteins immunoprecipitated from the cell lysate of GS115 expressing SAA1 (GS115-SAA1), suggesting that the binding between SAA1 and PDI was too weak that it could not be detected by mass spectrometry. Alternatively, there may be no direct interaction between SAA1 and PpDI in GS115-SAA1. These results could also be explained by the mode of binding between SAA1 and PpPDI as seen in the docking analysis, which showed that SAA1 could bind PpPDI from outside the U-shape structure. In comparison, the binding between PpPDI and Aβ42 or α-Syn could cause a steric effect leading to a longer retention of the substrates by PpPDI.

3.3 Computational analysis of the binding of PpPDI with three disulfide-free proteins

To further investigate the stabilities of the three protein complexes (PpPDI-Aβ42, PpPDI-α-Syn and PpPDI-SAA1), the root-mean-square deviations (RMSDs) of the skeleton carbon atoms of PpPDI from the three complexes were calculated for all simulations. The RMSD value of PpPDI in the PpPDI-Aβ42 complex was maintained in a relative equilibrium region during the whole 20 ns

simulations, suggesting the formation of a stable complex (Figure 4A). In the PpPDI-SAA1 complex, PpPDI exhibited a distinct fluctuation range when comparing the first half with the second half of the simulation, suggesting that there might be some uncertainty in the binding between PpPDI and SAA1 in the complex. In addition, the RMSD value of PpPDI in the PpPDI-α-Syn complex increased gradually as soon as the simulation began and then fluctuated in a relatively high equilibrium region, indicating that the complex was unstable during the simulation progress.

Root Mean Square Fluctuation (RMSF) was used to calculate the movement of single amino acid during the simulations. Proteins undergo significant structural changes during ligand binding, and so the average RMSF values obtained during the MD simulation were calculated to further explore the detailed structural changes occurring in PpPDI. Major fluctuations were found clustering around the a and b' domains of PpPDI in the case of the α-Syn-PpPDI and SAA1-PpPDI complexes (Figure 4B). In contrast to these observations, the fluctuation occurring in the Aβ42-PpPDI complex was minor and tended to stabilize at a relatively low equilibrium region. The structural changes in the a and b' domains of PpPDI could be more likely caused by the interference of binding between α-Syn/SAA1 and PpPDI (Figure 4B). According to the superimposition of the PpPDI-substrate protein complex structures (Fig. 4C), the three substrate-binding sites on PpPDI were relatively fixed at the end of the MD simulation. Although the binding of both Aβ and α-Syn to PpPDI involved the inner part of the U-shaped structure, the U-cleft of PpPDI only underwent minor distortion upon binding with either protein. On the contrary, the binding of SAA1 with PpPDI caused the U-shaped groove to open more widely upon binding with the b' and a' domains of PpPDI from the outside.

3.4 Changes in the proteomic profile of GS115-PpPDI expressing the amyloidogenic protein Aβ42 or SAA1.

A total of 237 Aβ42-interacting proteins were coimmunoprecipitated with Aβ42 in GS115 expressing Aβ (GS115-Aβ) and 95 in GS115 expressing both PpPDI and Aβ (GS115-PpPDI-Aβ) (Fig. 5A). By comparison, 103 and 189 SAA1-interacting proteins were coimmunoprecipitated with anti-SAA1 antibody in strain GS115-SAA1 and GS115-PpPDI-SAA1, respectively. PpPDI was present among the detected proteins from GS115-PpPDI expressing Aβ42 or SAA1. Interestingly, PpPDI was not detected in the cell lysate of GS115-SAA1 but was detected in the cell lysate of GS115-PpPDI-SAA1. This was consistent with our previous work on heterologous amyloidogenic protein expression in which the retention and secretion of SAA1 were found to be unaffected by the overexpression of PpPDI. It was also consistent with the result of the docking analysis.

Proteomics analysis identified 11 quantifiable proteins that were present in all samples (Fig. 5A). Interestingly, the genes coding for these proteins were found to be enriched in 34 basic biological processes, such as purine-containing compound biosynthesis (GO:0072522), ribose phosphate metabolism (GO:0019693), nucleoside phosphate biosynthesis (GO:1901293), nucleoside monophosphate metabolism (GO:0009123), and nucleoside triphosphate metabolism (GO:0009141). The detected cellular components, including cytosolic large ribosomal subunit (GO:0022625), phosphopyruvate hydratase complex (GO:0000015), mitochondrial proton-transporting ATP synthase complex, and catalytic core F(1) (GO:0000275) would warrant the preparation and maintenance of cellular activities (Fig. 5C). Interestingly, up to 33 proteins (circled by the red dotted line in Fig. 5A) were identified as being specifically belonging to GS115-PpPDI-Aβ when compared with the immunoprecipitated proteins identified from the cell extracts of GS115-Aβ, GS115-SAA1 and GS115-PpPDI-SAA1. As shown in Figure 5B, Go analysis of the 33 corresponding genes revealed an enrichment of these genes in canonical biological processes such as replicative cell aging (GO: 0001302), cellular carbohydrate catabolic process (GO: 0044275), cellular ion homeostasis (GO: 0006873) and regulation of response to a stimulus (GO:0048583), suggesting that PDI related regulation correlates with these biological processes and

molecular functions, leading to the elongated intracellular retention time of Aβ. For the category of molecular function, some genes were found to be significantly related to the enzymatic activity (GO: 0003824) and protein serine/threonine kinase activity (GO: 0004674).

More importantly, a number of heat shock proteins (Hsp) related to the protein quality control compartments (PQC) were found in the GS115-Aβ strain (Hsp12，Hsp42，Hsp60，Hsp82), while only Hsp12 was found in the GS115-PpPDI-Aβ, indicating that Aβ42 was spatially sequestered into dynamic, ER-anchored, structures called Q-bodies, whereas the insoluble Aβ42 aggregates were sequestered in the Insoluble Protein Deposit (IPOD) compartment. Interestingly, normal spatial quality control in the healthy cells of GS115-PpPDI-Aβ might be achieved by overexpressing PpPDI (Supplementary Table 4). In contrast, few proteins related to PQC in eukaryotic cells were found in the proteins immunoprecipitated from both GS115-SAA1 and GS115-PpPDI-SAA1 cell extracts.

3.5 Effect of PDI-overexpression on the proteomic profile of GS115-α-Syn.

Using anti-α-Syn antibody, a total of 576 and 62 α-Syn-interacting proteins were immunoprecipitated from the cell extracts of GS115-α-Syn and GS115-PpPDI-α-Syn, respectively (Fig. 6A). Proteomic analysis identified a total of 52 quantifiable proteins that were present specifically in the cell extract of GS115-PpPDI-α-Syn. The genes encoding these proteins were found to be significantly enriched in yeast reproduction-related biological processes or cellular components, such as cell budding (GO: 0007114) and mating projection tip (GO:0043332)(Fig. 6B), suggesting an increased *P. pastoris* reproduction rate promoted by PpPDI over-expression. The main genes involved were TAO3, SOG2, MYO2, SEC3 and PUF6. The intensity-based absolute quantification (iBAQ) of the amount of different common quantifiable immunoprecipitated proteins present in the cell lysates of both GS115-α-Syn and GS115-PpPDI-α-Syn is shown in Figure 6C. It is worth noting that a significantly higher amount of PpPDI was detected in the GS115-PpPDI-α-Syn cell extract than

in the GS115-α-Syn cell extract. In contrast, the other nine common proteins showed the same reverse trend since their levels were much higher in GS115-α-Syn than in GS115-PpPDI-α-Syn.

It is important to note that several key proteins related to PQC compartments in eukaryotic cells as well as ER-associated Q-bodies and degradation were found in the immunoprecipitated proteins from GS115-α-Syn: Hsp10, Hsp12, Hsp42, Hsp78, Hsp82, Hsp104, Ydj1, Sse1, Ubiquitin-activating enzyme, E3 ubiquitin-protein ligase and Ubiquitin-40S ribosomal protein S31. In contrast, no Hsp protein related to the PQC compartments was found in GS115-PpPDI-α-Syn**.** Only the ubiquitin-activating enzyme was found in GS115-PpPDI-α-Syn, indicating that overexpression of PpPDI led to a good spatial quality control system in cells of GS115-PpPDI-α-Syn (Supplementary Table 4).

4. Discussion

PDI catalyses the reduction, oxidation, or isomerization of disulfide bonds of its substrate proteins. It also acts as a disulfide bond-dependent and disulfide bond-independent molecular chaperone. An increasing number of studies have reported a link between the chemistry of disulfide and the pathogenesis of misfolded diseases [31]. However, the specific disulfide-free substrates of PDI in the ER have largely remained elusive, in part because of the transient nature of the PDI-substrate interaction. A previous study demonstrated that significant changes in the expression levels of exogenous amyloidogenic proteins in *Saccharomyces cerevisiae* was correlated with the disruption of Eps1, a member of the PDI family in yeast [32]. Considering the possible lethal effect of PDI-disruption in yeast, PpPDI was co-overexpressed with three amyloidogenic disulfide-free proteins in *P. pastoris* GS115. The results from protein biochemistry and molecular biology experiments suggested that overexpression of PpPDI affected the expression of three disulfide-free amyloidogenic proteins differently: it significantly increased the intracellular retention level of naturally disordered

amyloidogenic proteins (Aβ42 and α-Syn) but did not affect the secretion of the amyloidogenic protein SAA1.

A major finding of this study is that overexpression of PpPDI in *P. pastoris* could allow more disordered amyloidogenic proteins to be retained in the cell, thereby facilitating the proteins to fold into their correct structures. Moreover, the presence of PpPDI in the immunoprecipitated proteins of GS115-Aβ, GS115-PpPDI-Aβ, GS115-α-Syn and GS115-PpPDI-α-Syn but not in GS115-SAA1, together with the fact that the amount of PpPDI detected in GS115-PpPDI-α-Syn was higher than that detected in GS115-α-Syn (Fig. 6C) not only confirmed the involvement of PDI as an important molecular chaperone in the protein quality control system but also indicated that the binding between PpPDI and its disulfide-free substrates was substrate-dependent. It is well accepted that besides removing the misfolded proteins by degradation, a cell also strategically sequesters these proteins into transient or stable aggregates, often in defined cellular locations [33]. Since PDI is an ER-resident protein-folding catalyst, it is conceivable that when a naturally disordered protein fails to fold into its native state or the expression of the protein exceeds the folding capacity of the ER, the unfolded or aggregated proteins may start to accumulate in the ER. In the case of yeast, it always forms a membrane-bound ER-associated compartment (ERAC), which serves as a holding site before ER-associated degradation [34, 35].

To our knowledge, there has been no *in vivo* study investigating the mode of binding that occurs between PpPDI and its disulfide-free substrates. Our initial attempt to investigate the PDI-substrate interaction by performing co-IP only confirmed a PpPDI-Aβ42 interacting complex in GS115-PpPDI-Aβ. To overcome this challenge we have adapted and developed a combined strategy in which the interaction and specific mode of binding between PpPDI and each of the three substrate proteins were first explored by molecular docking and simulations, and the interaction of PpPDI with its

substrates was then examined by Co-IP and LC-MS/MS. The computational findings in this study were consistent with molecular findings. Firstly, amyloidogenic Aβ42 was more likely to accumulate intracellularly in the PpPDI-overexpressing GS115 strain. This was consistent with the MD simulation result which showed the formation of a stable complex between PpPDI and Aβ42, although this experiment should be repeated with a longer simulation time. This indicated that Aβ42 may enter the U-shaped cleft of PpPDI and become trapped in the U-shaped groove because of the steric hindrance. Secondly, in the case of the α-Syn-PpPDI complex, major fluctuations were found clustering around the a and b' domains of PpPDI, indicating the dynamic interferences in the binding between α-Syn and PpPDI, consistent with the proteomic analysis which detected a significantly higher amount of PpPDI in the extract of GS115-PpPDI-α-Syn than in the extract of GS115-α-Syn cell. Such observation was in contrast to the reverse trend observed for the other nine common proteins (Fig. 6A). Finally, expression analysis showed that amyloidogenic SAA1 was more readily secreted in both GS115 and GS115-PDI, consistent with the pattern of PpPDI-SAA1complex obtained by MD simulation, which effectively demonstrated that the instability of the PpPDI-SAA1 complex might have been conferred by the extensive flexible motion of PpPDI caused by of SAA1. Hopefully, this combined strategy of methodology could be adapted for most other PDI substrates and be applied to other molecular chaperones as well.

We have generated three different patterns of PpPDI-substrate complexes, suggesting that multiple modes of binding might exist for the binding between PpPDI and its amyloidogenic protein substrates, and this could represent the different specificities of PpPDI towards its substrates. The spatial shape of the U-shape structure in PpPDI would determine its selection and recognition of substrates. Thus, proteins with hydrophobic properties, especially those with smaller hydrophobic cyclotron radius, are more likely to bind to PpPDI and be captured, retained and folded by PpPDI. In

the case of the SAA1-PpPDI complex, the binding of SAA1 with PpPDI would consist of a form of continuous association and dissociation, thus providing more opportunities for other PDI substrates to bind. Consequently, overexpression of PpPDI did not increase the expression or retention level of SAA1. In contrast, the binding of Aβ42 to PpPDI resulted in Aβ42 being more closely bound to the hydrophobic pocket of PpPDI, thereby significantly increased the intracellular retention of Aβ42 in GS115-PpPDI-Aβ (Figure 3). The docking and simulation studies of PpPDI dimer-substrate complexes were not carried out in this work because the existence of PpPDI dimer in ER of *P. pastoris* was uncertain.

Finally, a better understanding of the spatial quality control in healthy cells can help us understand the nature of the problems that arise in amyloid diseases, including Alzheimer's, Parkinson's, and Huntington's diseases, amyotrophic lateral sclerosis (ALS) and many others [16, 35]. Proteomic analysis of GS115-Aβ, GS115-PpPDI-Aβ, GS115-α-Syn and GS115-PpPDI-α-Syn revealed no Hsp family member protein from the PQC compartments in the case of GS115-PpPDI-α-Syn, while only a few members were found in GS115-PpPDI-Aβ strain, respectively. Accordingly, few PQC compartment related proteins were identified in the two PpPDI overexpressing strains, implying a healthy intracellular cell condition in GS115-PpPDI-Aβ and GS115-PpPDI-α-Syn. In addition, only ubiquitin-activating enzyme was found in GS115-PpPDI-α-Syn, while ubiquitin-activating enzyme, E3 ubiquitin-protein ligase, ubiquitin-40S ribosomal protein S31 were all identified in GS115-α-Syn, consistent with previous reports of alternative degradation pathways of α-Syn, with soluble species of the same protein degraded via the proteasome [36-38].

In recent years, since pharmacological control of the proteostasis network via targeting to chaperones could be a potential therapeutic procedure to improve the quality control system in our body, more attention has been devoted to the research of molecular chaperone drugs and related topics

[33]. The co-expression of molecular chaperone genes with the *PDI* gene has been a major strategy for the genetic improvement of ER-resident proteins [39, 40]. In this study, the co-overexpression of three disulfide-free amyloidogenic proteins of PpPDI in *P. pastoris* was found to attenuate the need for cellular machinery that sequesters surplus and misfolded proteins, thus alleviating the toxicity of these deposits. By considering its essential role in ER proteostasis, PDI, therefore, merits consideration as a potential therapeutic molecular chaperone drug candidate for both Parkinson's disease and Alzheimer's disease.

5. Conflict of interest

N.G.N.M. is named as the inventor on a UK patent held by the University of Roehampton for the use of kissorphin peptides to treat Alzheimer's disease, Creutzfeldt-Jakob disease or diabetes mellitus (Publication Numbers: GB2493313 B); under the University of Roehampton rules he could benefit financially if the patent is commercially exploited. The reference for this patent is: Milton, N. (2017) Kissorphin peptides for use in the treatment of Alzheimer's disease, Creutzfeldt-Jakob disease or diabetes mellitus. United Kingdom Patent Publication Number GB 2493313 (B). N.G.N.M. is also a shareholder and director of NeuroDelta Ltd (UK Company No: 06222473; http://www.neurodelta.uk).

6. References

[1] J. Kemmink, N.J. Darby, K. Dijkstra, M. Nilges, T.E. Creighton, The folding catalyst protein disulfide isomerase is constructed of active and inactive thioredoxin modules, Curr. Biol. 7(4) (1997) 239-45.

[2] C.C. Wang, C.L. Tsou, Protein disulfide isomerase is both an enzyme and a chaperone, FASEB J. 7(15) (1993) 1515-7.

[3] P. Klappa, H.C. Hawkins, R.B. Freedman, Interactions between protein disulphide isomerase and peptides, Eur. J. Biochem. 248(1) (1997) 37-42.

[4] A.Y. Denisov, P. Maattanen, C. Dabrowski, G. Kozlov, D.Y. Thomas, K. Gehring, Solution

structure of the bb' domains of human protein disulfide isomerase, FEBS J. 276(5) (2009) 1440-9.
[5] L.J. Byrne, A. Sidhu, A.K. Wallis, L.W. Ruddock, R.B. Freedman, M.J. Howard, R.A. Williamson, Mapping of the ligand-binding site on the b' domain of human PDI: interaction with peptide ligands and the x-linker region, Biochem. J. 423(2) (2009) 209-17.
[6] C. Wang, J. Yu, L. Huo, L. Wang, W. Feng, C.C. Wang, Human protein-disulfide isomerase is a redox-regulated chaperone activated by oxidation of domain a', J. Biol. Chem. 287(2) (2012) 1139-49.
[7] A.G. Irvine, A.K. Wallis, N. Sanghera, M.L. Rowe, L.W. Ruddock, M.J. Howard, R.A. Williamson, C.A. Blindauer, R.B. Freedman, Protein disulfide-isomerase interacts with a substrate protein at all stages along its folding pathway, PLoS. One 9(1) (2014) e82511.
[8] C. Wang, W. Li, J. Ren, J. Fang, H. Ke, W. Gong, W. Feng, C.C. Wang, Structural insights into the redox-regulated dynamic conformations of human protein disulfide isomerase, Antioxid. Redox Sign. 19(1) (2013) 36-45.
[9] N.J. Darby, E. Penka, R. Vincentelli, The multi-domain structure of protein disulfide isomerase is essential for high catalytic efficiency, J. Mol. Biol. 276(1) (1998) 239-47.
[10] F. Hatahet, L.W. Ruddock, Protein disulfide isomerase: a critical evaluation of its function in disulfide bond formation, Antioxid. Redox Sign. 11(11) (2009) 2807-50.
[11] Z. Li, A. Moy, S.R. Gomez, A.H. Franz, J. Lin-Cereghino, G.P. Lin-Cereghino, An improved method for enhanced production and biological activity of human secretory leukocyte protease inhibitor (SLPI) in *Pichia pastoris*, Biochem. Biophys. Res. Commun. 402(3) (2010) 519-24.
[12] M. Inan, D. Aryasomayajula, J. Sinha, M.M. Meagher, Enhancement of protein secretion in *Pichia pastoris* by overexpression of protein disulfide isomerase, Biotechnol. Bioeng. 93(4) (2006) 771-8.
[13] C.W. Tsai, P.F. Duggan, R.L. Shimp, Jr., L.H. Miller, D.L. Narum, Overproduction of *Pichia pastoris* or Plasmodium falciparum protein disulfide isomerase affects expression, folding and O-linked glycosylation of a malaria vaccine candidate expressed in *P. pastoris*, J. Biotechnol. 121(4) (2006) 458-70.
[14] L.M. Damasceno, K.A. Anderson, G. Ritter, J.M. Cregg, L.J. Old, C.A. Batt, Cooverexpression of chaperones for enhanced secretion of a single-chain antibody fragment in *Pichia pastoris*, Appl. Microbiol. Biotechnol. 74(2) (2007) 381-9.
[15] E. Lee, D.H. Lee, Emerging roles of protein disulfide isomerase in cancer, BMB Rep. 50(8)

(2017) 401-410.
[16] E.R. Perri, C.J. Thomas, S. Parakh, D.M. Spencer, J.D. Atkin, The Unfolded Protein Response and the Role of Protein Disulfide Isomerase in Neurodegeneration, Front. Cell. Dev. Biol. 3 (2015) 80.
[17] R. Kumar, P. Kumar, Yeast-based vaccines: New perspective in vaccine development and application, FEMS Yeast Res. 19(2) (2019).
[18] J.M. Zolezzi, S. Bastias-Candia, M.J. Santos, N.C. Inestrosa, Alzheimer's disease: relevant molecular and physiopathological events affecting amyloid-beta brain balance and the putative role of PPARs, Front. Aging. Neurosci. 6 (2014) 176.
[19] D.J. Selkoe, J. Hardy, The amyloid hypothesis of Alzheimer's disease at 25 years, EMBO Mol. Med. 8(6) (2016) 595-608.
[20] J. Trambauer, A. Fukumori, H. Steiner, Pathogenic Abeta generation in familial Alzheimer's disease: novel mechanistic insights and therapeutic implications, Curr. Opin. Neurobiol. 61 (2020) 73-81.
[21] J. Lu, Y. Yu, I. Zhu, Y. Cheng, P.D. Sun, Structural mechanism of serum amyloid A-mediated inflammatory amyloidosis, Proc. Natl. Acad. Sci. U S A 111(14) (2014) 5189-94.
[22] A. Husebekk, B. Skogen, G. Husby, G. Marhaug, Transformation of amyloid precursor SAA to protein AA and incorporation in amyloid fibrils *in vivo*, Scand. J Immunol. 21(3) (1985) 283-7.
[23] S. Claus, K. Meinhardt, T. Aumuller, I. Puscalau-Girtu, J. Linder, C. Haupt, P. Walther, T. Syrovets, T. Simmet, M. Fandrich, Cellular mechanism of fibril formation from serum amyloid A1 protein, EMBO Rep. 18(8) (2017) 1352-1366.
[24] M. Yang, Y. Liu, J. Dai, L. Li, X. Ding, Z. Xu, M. Mori, H. Miyahara, J. Sawashita, K. Higuchi, Apolipoprotein A-II induces acute-phase response associated AA amyloidosis in mice through conformational changes of plasma lipoprotein structure, Sci. Rep. 8(1) (2018) 5620.
[25] E. Malle, S. Sodin-Semrl, A. Kovacevic, Serum amyloid A: an acute-phase protein involved in tumour pathogenesis, Cell Mol. Life Sci. 66(1) (2009) 9-26.
[26] Y.C. Wong, D. Krainc, alpha-synuclein toxicity in neurodegeneration: mechanism and therapeutic strategies, Nat. Med. 23(2) (2017) 1-13.
[27] R. Guerrero-Ferreira, L. Kovacik, D. Ni, H. Stahlberg, New insights on the structure of alpha-synuclein fibrils using cryo-electron microscopy, Curr. Opin. Neurobiol. 61 (2020) 89-95.
[28] A. Warsame, R. Vad, T. Kristensen, T.B. Oyen, Characterization of a gene encoding a *Pichia*

pastoris protein disulfide isomerase, Biochem. Biophys. Res. Commun. 281(5) (2001) 1176-82.
[29] Y. Perez-Riverol, A. Csordas, J. Bai, M. Bernal-Llinares, S. Hewapathirana, D.J. Kundu, A. Inuganti, J. Griss, G. Mayer, M. Eisenacher, E. Perez, J. Uszkoreit, J. Pfeuffer, T. Sachsenberg, S. Yilmaz, S. Tiwary, J. Cox, E. Audain, M. Walzer, A.F. Jarnuczak, T. Ternent, A. Brazma, J.A. Vizcaino, The PRIDE database and related tools and resources in 2019: improving support for quantification data, Nucleic Acids Res. 47(D1) (2019) D442-D450.
[30] X. Zhou, X. Lu, S. Qin, L. Xu, X. Chong, J. Liu, P. Yan, R. Sun, I.P. Hurley, G.W. Jones, Q. Wang, J. He, Is the absence of alpha-helix 2 in the appendant structure region the major contributor to structural instability of human cystatin C? J. Biomol. Struct. Dyn. 37(17) (2019) 4522-4527.
[31] M. Okumura, K. Noi, S. Kanemura, M. Kinoshita, T. Saio, Y. Inoue, T. Hikima, S. Akiyama, T. Ogura, K. Inaba, Dynamic assembly of protein disulfide isomerase in catalysis of oxidative folding, Nat. Chem. Biol. 15(5) (2019) 499-509.
[32] J. He, T. Sakamoto, Y. Song, A. Saito, A. Harada, H. Azakami, A. Kato, Effect of EPS1 gene deletion in *Saccharomyces cerevisiae* on the secretion of foreign proteins which have disulfide bridges, FEBS Lett. 579(11) (2005) 2277-83.
[33] D. Balchin, M. Hayer-Hartl, F.U. Hartl, *In vivo* aspects of protein folding and quality control, Science 353(6294) (2016) aac4354.
[34] P. Yu, Q. Zhu, K. Chen, X. Lv, Improving the secretory production of the heterologous protein in *Pichia pastoris* by focusing on protein folding, Appl. Biochem. Biotechnol. 175(1) (2015) 535-48.
[35] E.M. Sontag, W.I.M. Vonk, J. Frydman, Sorting out the trash: the spatial nature of eukaryotic protein quality control, Curr. Opin. Cell. Biol. 26 (2014) 139-146.
[36] E. Cohen, J. Bieschke, R.M. Perciavalle, J.W. Kelly, A. Dillin, Opposing activities protect against age-onset proteotoxicity, Science 313(5793) (2006) 1604-10.
[37] K.B. Kruse, J.L. Brodsky, A.A. McCracken, Autophagy: an ER protein quality control process, Autophagy 2(2) (2006) 135-7.
[38] J.L. Webb, B. Ravikumar, J. Atkins, J.N. Skepper, D.C. Rubinsztein, Alpha-Synuclein is degraded by both autophagy and the proteasome, J. Biol. Chem. 278(27) (2003) 25009-13.
[39] A.J. McClellan, M.D. Scott, J. Frydman, Folding and quality control of the VHL tumor suppressor proceed through distinct chaperone pathways, Cell 121(5) (2005) 739-48.
[40] D. Kaganovich, R. Kopito, J. Frydman, Misfolded proteins partition between two distinct

quality control compartments, Nature 454(7208) (2008) 1088-95.

7. Figure legends

Figure 1. Structure of yeast PDI (PDB ID: 2B5E). PyMOL software was used to remove the water molecules and other ligands from the protein structure and to change the color of the structure. The flexible junction zone x is located between domains b' and a', the C-terminal extension (red) contains the (K / H) DEL retention signal of the ER.

Figure 2. Analysis of disulfide-free proteins expressed in *P. pastoris*. (A) Western blot analysis of Aβ42 from the cell extract. Lane 1, *P. pastoris* GS115; Lanes 2, *P. pastoris* GS115-PpPDI; Lane 3, Aβ42 in GS115-Aβ cell extract; lanes 4, Aβ42 in GS115-PpPDI-Aβ cell extract. The entire blot was treated by anti-Aβ42 antibody. (B) Western blot analysis of *P. pastoris* GS115 cell extracts. Lane 1, GS115; Lanes 2, GS115 overexpressing PpPDI; Lane 3, GS115 expressing α-Syn; lanes 4, GS115 expressing both PpPDI and α-Syn. The entire blot was treated with an anti-α-Syn antibody. Western blot analysis of SAA1 from the culture supernatant (C) and from the cell extract (D) of *P. pastoris* GS115-SAA1 or GS115-PpPDI-SAA1 induced with Methanol for 1, 2 and 3 days.

Figure 3. Docking analysis of the binding of PpPDI with the three amyloidogenic disulfide-free proteins. Residues involved in the binding between Aβ42 (yellow) and PpPDI (cyan) (A) and between α-Syn (gold) and PpPDI (B). Red lines indicate H-bonds. No hydrogen bond was involved in the binding between SAA1 (green) and PpPDI (C). Residues participated in hydrophobic interaction are shown in the Supplementary Table 3.

Figure 4. (A) RMSDs of the Cα-positions of PpPDI in three protein complexes during the 20 ns simulations. (B) RMSF trajectory per PpPDI residue during the period of MD simulations. (C) Superimposition of PpPDI-substrate complex structures at the beginning (PpPDI shown in pink,

substrate protein shown in green) and at the end of the MD simulations (PpPDI shown in yellow, substrate protein shown in blue).

Figure 5. Changes in the proteomic profile of GS115-PpPDI expressing the Aβ42 or SAA1. (A) Venn diagram depicting the total number of proteins that were co-precipitated with Aβ42 from the cell extracts of GS115-Aβ42 (GA, shown in blue) and GS115-PpPDI- Aβ (GPA, shown in yellow), or those that were co-precipitated with SAA1 from the cell extracts of GS115-SAA1 (GS, shown in flesh red) and GS115-PpPDI-SAA1 (GPS, shown in green). (B) Gene ontology (GO) enrichment analysis showing the functions of the 33 specific proteins immunoprecipitated from the cell extract of GPA with anti-Aβ42 antibody and identification of the canonical pathways participated by these proteins. The color intensity in the heat map diagram indicates the significance of GO term enrichment, presented as $-\log_{10}$ (P-value). Hierarchical clustering analysis was used to group the GO terms based on the p-value of enrichment. (C) GO enrichment analysis of the 11 common proteins immunoprecipitated from the cell extracts with either anti-Aβ42 or anti-SAA1 antibody and canonical pathways involved for these proteins were identified.

Figure 6. Effect of PDI-overexpression on the proteomic profile of GS115-α-Syn. (A) Venn diagram depicting the total number of proteins that were immunoprecipitated from GS115-α-Syn and GS115-PpPDI-α-Syn cell extracts by co-IP carried out with an anti-α-Syn antibody. (B) GO enrichment analysis of the proteins that were found to interact with α-Syn and identification of the canonical pathways for these proteins. (C) Quantitative determination of the amount of different common quantifiable immunoprecipitated proteins present in the cell lysates of GS115-α-Syn and GS115-PpPDI-α-Syn.

8. Figures

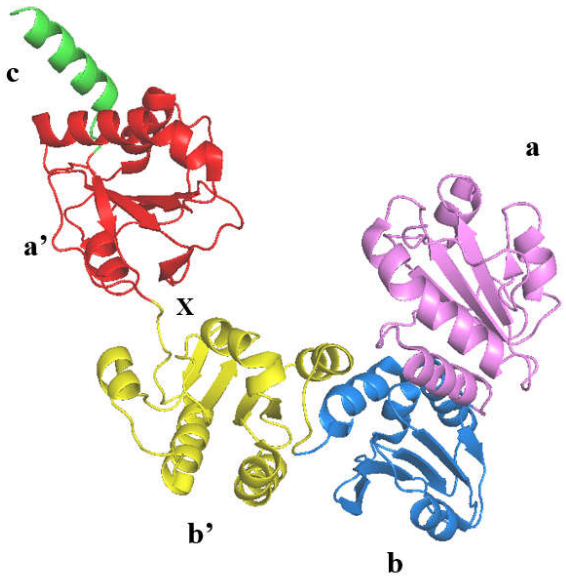

Figure 1.

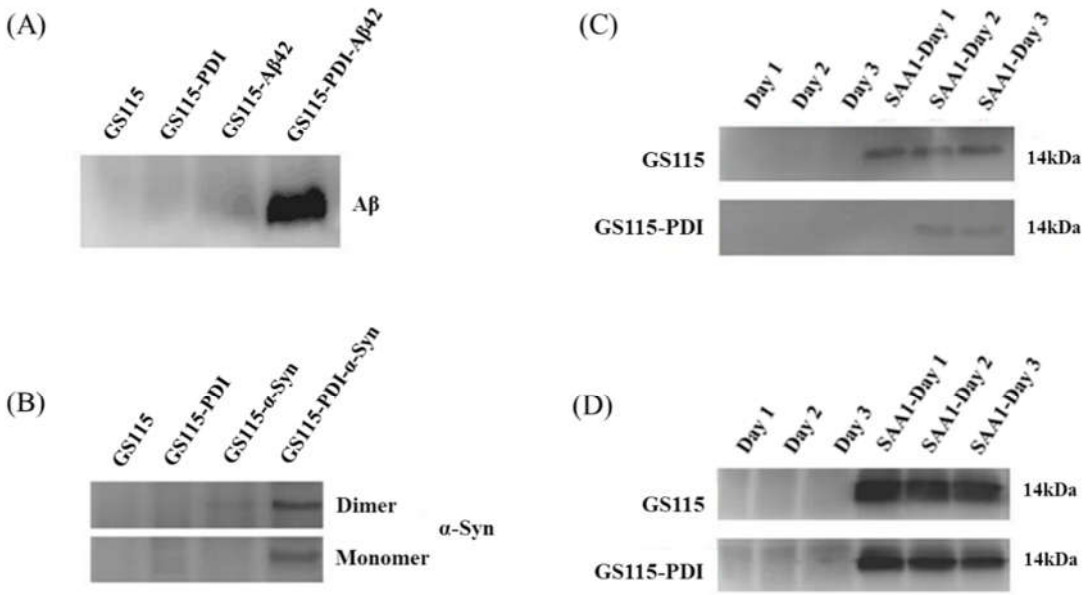

Figure 2.

(A)

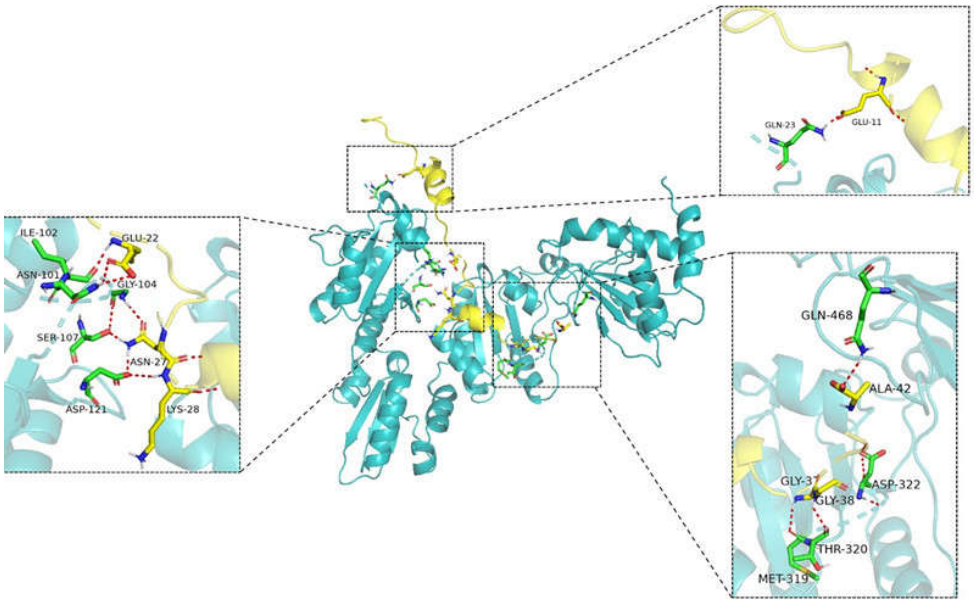
GLN-23
GLU-11
ILE-102
GLU-22
ASN-101
GLY-104
SER-107
ASN-27
ASP-121
LYS-28
GLN-468
ALA-42
GLY-37
ASP-322
GLY-38
THR-320
MET-319

Figure 3 (A)

(B)

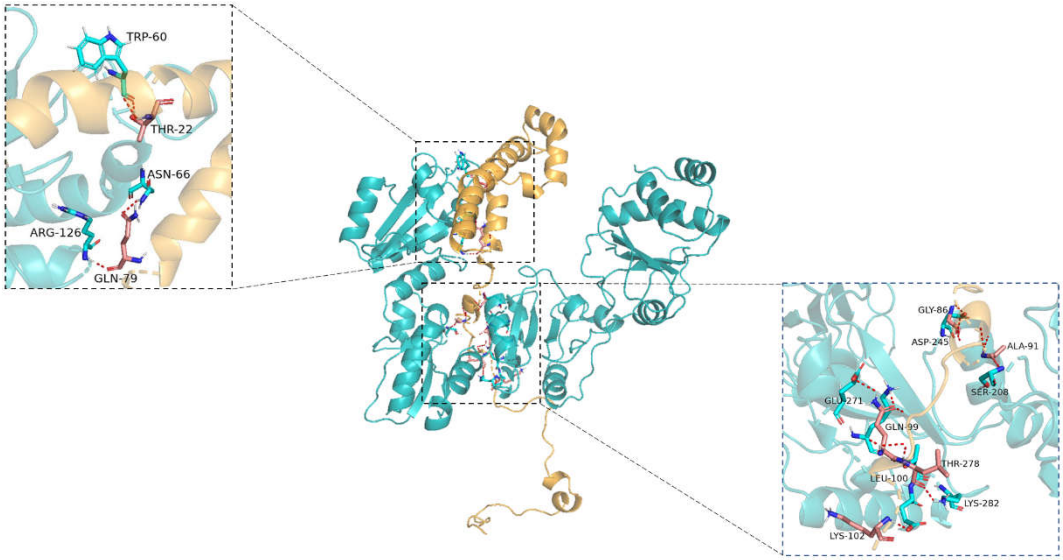

(C)

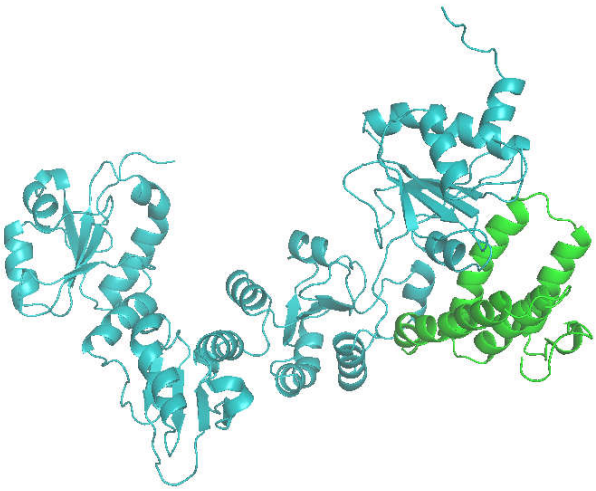

Figure 3 (B) &(C)

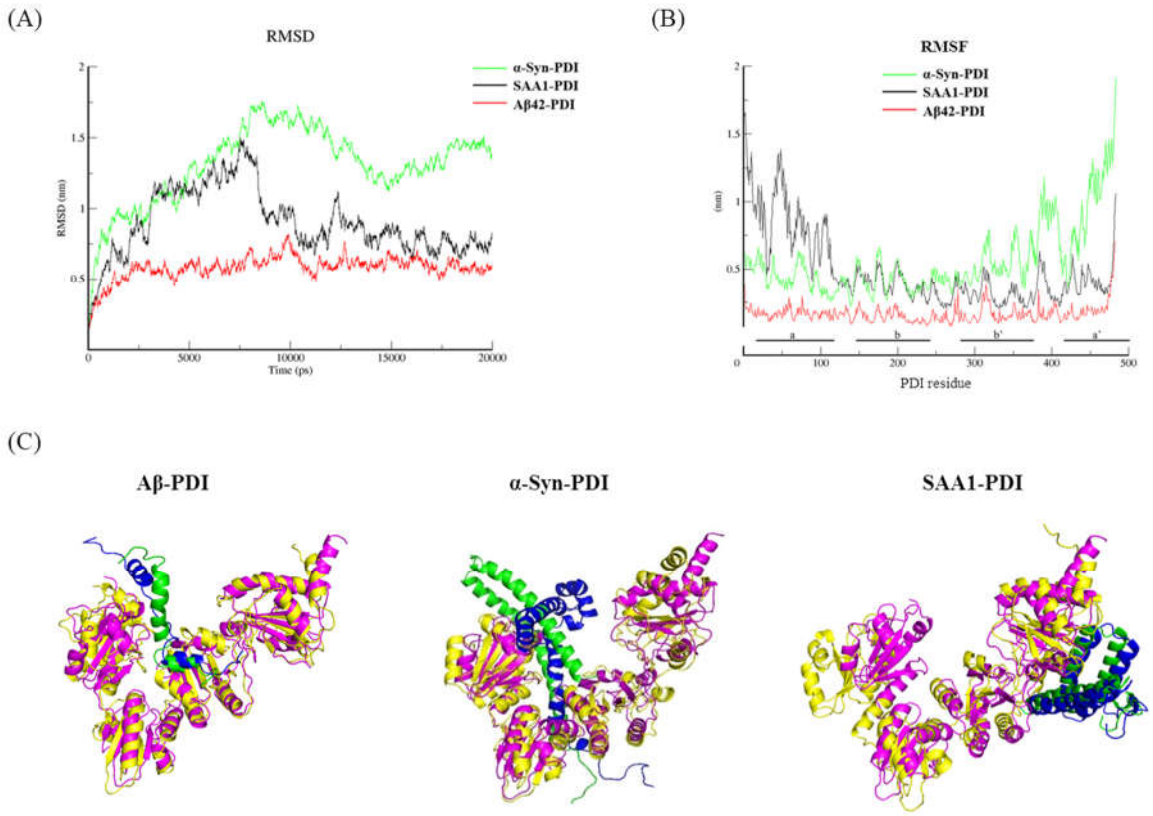
(A)
RMSD
α-Syn-PDI
SAA1-PDI
Aβ42-PDI
RMSD (nm)
Time (ps)
(B)
RMSF
α-Syn-PDI
SAA1-PDI
Aβ42-PDI
(nm)
a
b
b'
a'
PDI residue
(C)
Aβ-PDI
α-Syn-PDI
SAA1-PDI

Figure 4.

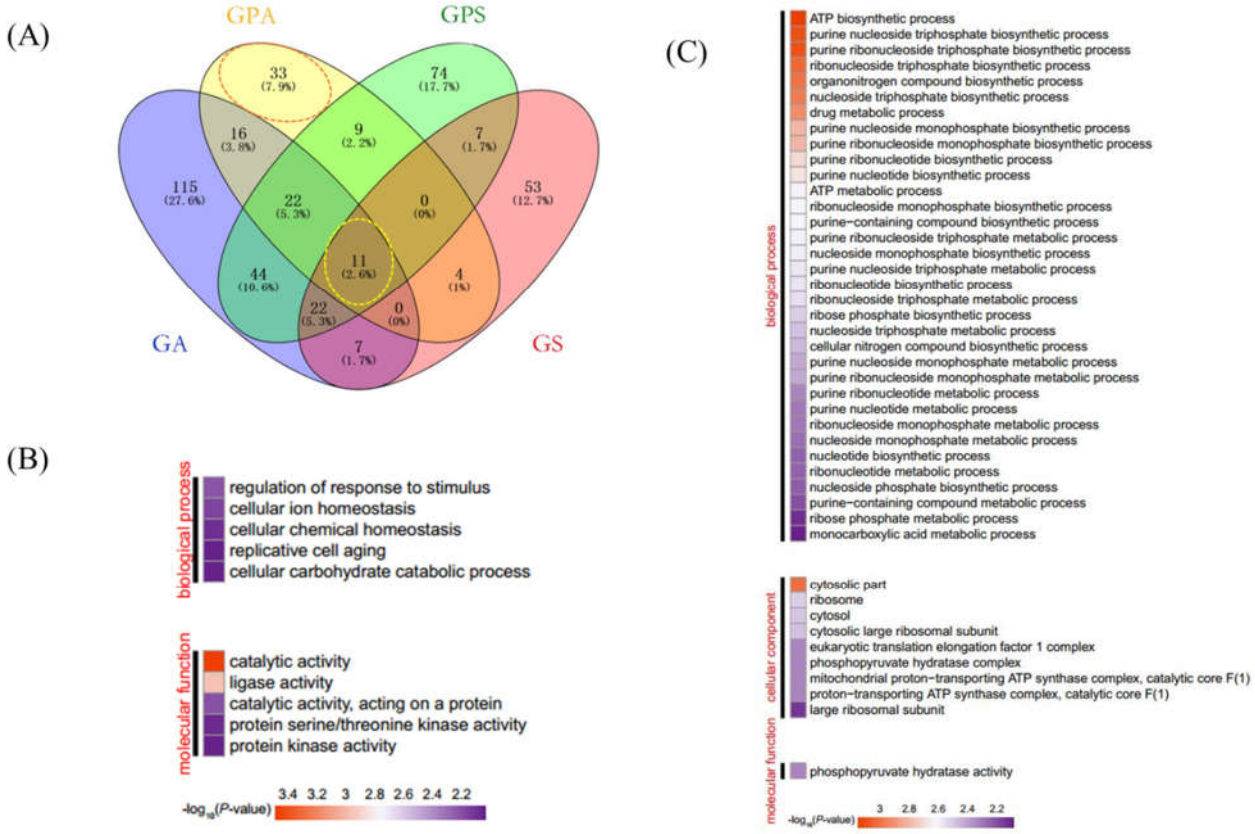

Figure 5.

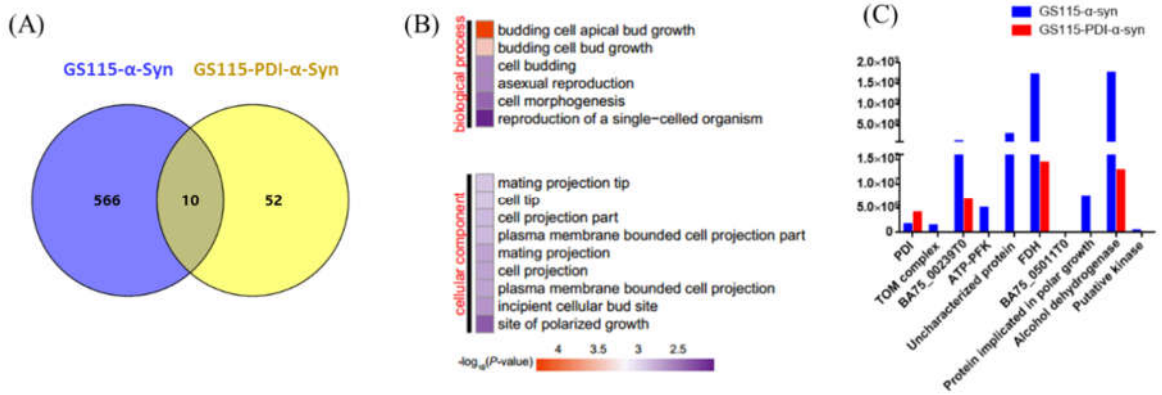

Figure 6.